NOTICE CONCERNING COPYRIGHT RESTRICTIONS

Hydrothermal Alteration and Evolution of the Bulalo Geothermal Field, Philippines

James Stimac[1], Joe Moore[2], and Jefferson Latayan[3]

[1]Chevron Geothermal, Jakarta, Indonesia
[2]Energy & Geoscience Institute, Salt Lake City, Utah
[3]University of the Philippines, Manila, Philippines

ABSTRACT

The Bulalo geothermal system, Philippines, is characterized by broadly distributed alteration related to multiple episodes of shallow igneous intrusion and hydrothermal fluid circulation. The most recent hydrothermal event is associated with the extrusion of dacite domes <22,000 years ago. At depth, high-temperature phyllic (sericite-quartz-pyrite) and propylitic (epidote-chlorite-quartz-pyrite) assemblages dominate. Anhydrite-bearing phyllic assemblages and advanced argillic alteration (pyrophyllite-type) are locally present in the contact region of intrusions emplaced deep on the W and SSW margins of the field. In the upper part of the system, smectite-and interlayered illite-smectite- and chlorite-smectite-bearing rocks form an impermeable cap that deepens and thickens outward from the region of upflow. Calcite is locally abundant within the clay cap and on the E and SE margin of the system, where noncondensable gas concentrations are highest. Vein filling sequences and fluid inclusion measurements highlight the effects of the initial heating, catastrophic decompression and boiling, and later inflow of cooler marginal fluids.

Introduction

The Bulalo geothermal system, located on Luzon Island in the Philippines, hosts hydrothermal alteration assemblages that bear a strong relationship to the distribution of major structures, reservoir lithologies and the distribution of shallow (<4 km) intrusions. This paper briefly documents the mineral paragenesis and thermal history of the Bulalo geothermal system based on petrographic and fluid inclusion studies of the reservoir rocks and surrounding areas (Figures 1 and 2). Bulalo lies on the SE flank of Mt. Makiling, an extinct stra-

tocone and dome complex, and astride two satellite dacite domes that were recently dated at <22,000 years old (Vogel et al., 2006). Uranium/Lead SHRIMP dates of zircon demonstrate that more than 2 km of volcanic and volcaniclastic sedimentary rock, comprising andesitic stratocone, stratocone flank, and thick caldera-related rhyolitic tuff sequences, has accumulated in the area in the past 500,000 years (Dimabuyu et al., 2005). The upper portion of this rapidly emplaced volcanic pile retains relatively high porosity despite hydrothermal alteration, and locally exerts a strong control on permeability and fluid flow.

The geothermal reservoir consists of a structurally-controlled central upflow of relatively high permeability surrounded by hot, lower permeability rocks. A secondary and smaller region of upflow has also been identified in the SE (Golla et al., 2001). Prior to exploitation, high-temperature fluids outflowed to the north, west and southwest along litho-
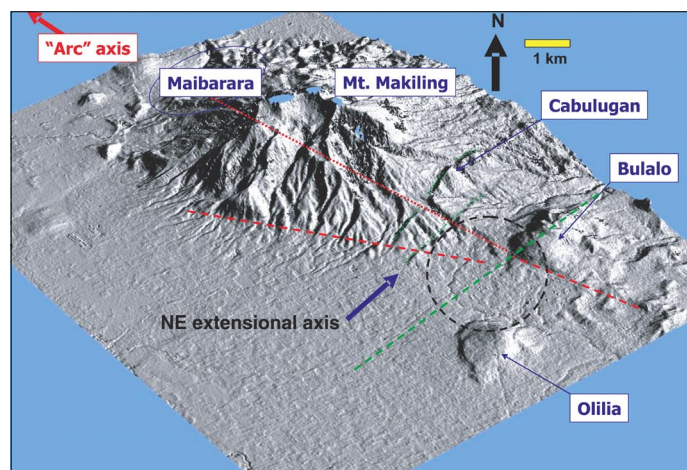
Figure 1. Location of the Bulalo geothermal field within the Macolod Corridor, a broad zone of extensional faulting oriented transverse to the trend of oppositely-dipping subduction zones to the north and south. The commercial reservoir (black dashed line) is associated with the dacitic Bulalo and Olilia domes on the flank of Mt. Makiling, an eroded composite volcano.
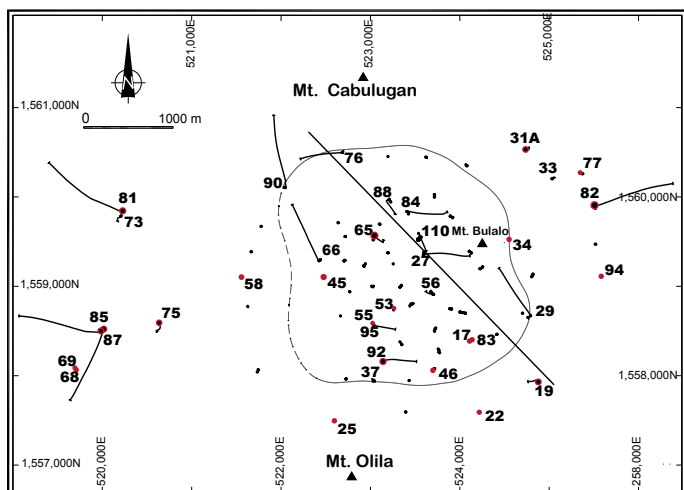
Figure 2. Map of the Bulalo geothermal field. The commercial reservoir boundary is indicated by the solid/dashed line. The trajectories and wellhead locations of wells sampled for petrologic and fluid inclusion studies are shown in black. Wellheads shown in red denote wells that encountered intrusions. For clarity, the well courses are not illustrated. The solid line shows the location of the NW-SE cross-section shown in Figure 3.

logically and structurally controlled pathways (Abrigo et al., 2004). Bulalo has some features in common with geothermal systems related to continental extension such as those in New Zealand or Kenya by virtue of its location in the extensional Macolod Corridor (Förster et al., 1990). Like other two-phase geothermal systems such as Olkaria, Kenya, there are no associated hot springs (Hochstein and Browne, 2000), but fumaroles and altered ground are present in an area of proximal outflow to the N and NW.

Bulalo currently has an installed capacity of 426 MWe. The commercial reservoir is a high-temperature (340 to 260°C) liquid-dominated resource that developed extensive zones of two-phase production under exploitation (Clemente and Villadolid-Abrigo, 1993). The central upflow zone has a relatively low salinity (Cl generally <2800 mg/kg) and a very low noncondensable gas (NCG) content (generally <0.5 wt% in steam) (Golla et al., 2001). In contrast, the SE portion of the field has higher salinity (up to 4500 mg/kg Cl) and NCG concentrations (2 to 3 wt% in steam). Chloride and NCG patterns for early production wells can be smoothly contoured but there are steep gradients between the SE and central zones that are mirrored in the abundances of epidote and calcite (Figure 3). Changes in reservoir Cl and NCG concentrations during exploitation indicate that the deep marginal fluids (temperature from 216-293°C, 1500 ppm reservoir Cl, 0.4 wt% NCG), which flowed outward from the system, provides the dominant recharge component under exploitation (Abrigo et al., 2004). Gas chemistry is typical of andesitic-hosted liquid-dominated systems except that the NH_3 concentration is relatively low. Low NH_3 suggests that organic-rich sedimentary rocks are rare in the zone of metamorphism surrounding the heat source. This is consistent with the complete absence of sedimentary rocks in cores and cuttings to depths where plutonic rocks begin to dominate at elevations between -2000 and -3000 m above sea level (asl). Helium isotopes ($^3He/^4He$ = 6.8 Ra),
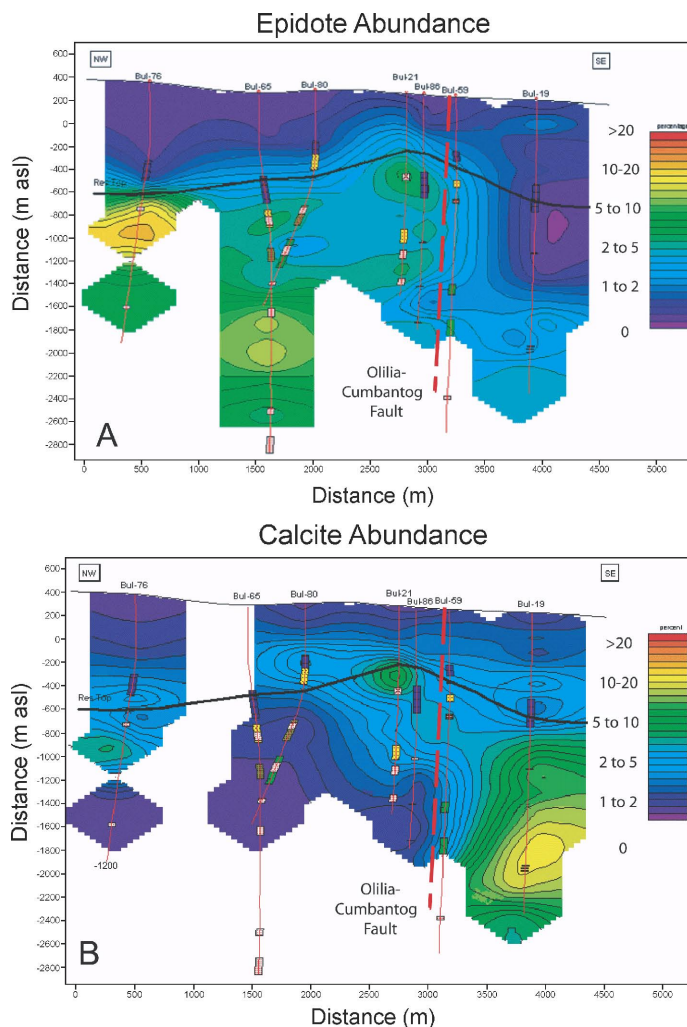
Figure 3. NW-SE cross section with the contoured abundance of epidote (A) and calcite (B). An antithetic relationship and sharp boundary between zones of maximum abundance is evident where the section crosses the Olilia-Cumbantog fault (between Bul-86 and Bul-59). The solid black line marks the top of the reservoir. Elevations in m asl. The color scale indicates relative mineral abundance and ranges from absent (purple) to very abundant (>20 vol%).

carbon isotopes (-2.7 to 4.1 per mil) and $CO_2/^3He$ ratios of 1 x10^{10} have strong magmatic signatures, but D and ^{18}O show only minor shifts from the local meteoric water composition (Hilton et al., 2004).

Distribution of Alteration Assemblages

The Bulalo geothermal system is characterized by broadly distributed hydrothermal alteration that is spatially associated with a variety of shallow igneous intrusions in its deeper portions. Although the top of the reservoir deepens on its sides and permeability is below commercial limits, only high-temperature alteration at depth was encountered in all but a few wells on the far margins of the drilled area (Clemente and Villadolid-Abrigo, 1993; Golla et al., 2001).

The general distribution of mineral assemblages was described by Golla et al. (2001). They showed that the clay-rich
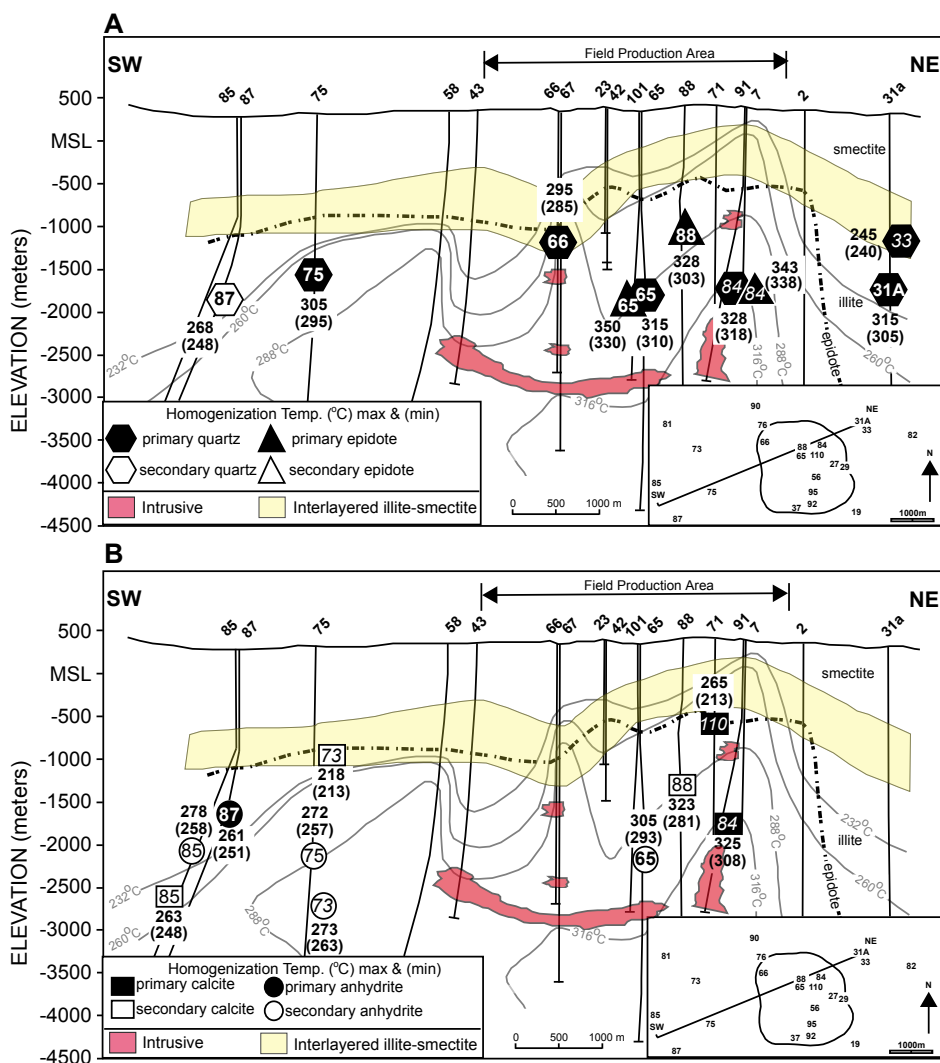
Figure 4. NE-SW cross section of Bulalo (see inset). The productive portion of the field and the locations of wells sampled for petrologic and fluid inclusion studies are shown in the inset. The shallowest occurrence of epidote marks the approximate top of the reservoir. Measured temperatures are shown by the light lines. Maximum and minimum temperatures of fluid inclusions trapped in minerals deposited during paragenesis 1 (4A) and 2 (4B) are in bold. (A) Temperatures of epidote- and quartz-hosted fluid inclusions. (B) Temperatures of calcite- and anhydrite-hosted fluid inclusions. Symbols in italics denote data from wells not shown on the cross section. Elevations in m asl.

lower permeability. The zone of abundant calcite thickens to at least -3000 m asl to the SE across the Olilia-Cumbantog fault (Figure 3B). The correspondence between abundant deep calcite and high noncondensable gas contents (mainly CO_2), which would stabilize calcite over epidote or wairakite has been noted by several workers (Clemente, 1987; Golla et al., 2001; Abrigo et al., 2004).

Extensive phyllic (chlorite-sericite-quartz-anhydrite-pyrite) and local advanced argillic alteration (pyrophyllite-type) occur deep on the W (Bul-85, 75, 73, 58) and SSW margins of the field (Bul-69, 68) in the contact regions of larger granitic to dioritic intrusions. Advanced argillic alteration is restricted to narrow zones of pervasive sericitic or phyllic alteration that is cut by late-stage veins of anhydrite. Pyrophyllite forms at a moderate pH (4-5) and temperatures >250°C. Both the occurrence of anhydrite as an alteration product of the phenocrysts associated with phyllic assemblages and the deposition of pyrophyllite suggests interactions with magmatic fluids (Reyes, 1990; Hedenquist et al., 1998). Reyes (1990) noted that anhydrite is commonly the dominant Ca-bearing phase deep in Philippine geothermal systems (e.g., Mahiao-Sambaloran sector of Tongonan), whereas calcite is dominant at shallower levels.

Intrusions and their Contact Regions

Composite intrusions and related dikes and sills are common in the deepest wells of Bulalo, especially on the W, SW and E sides of the commercial reservoir (Table 1, overleaf, and Figure 2). The plutonic rocks are generally coarser-grained than the lavas, have late-stage groundmass quartz and K-feldspar, and have distinctive primary mineral assemblages that include oligoclase, pyroxene, K-feldspar, biotite and magnetite. Secondary K-feldspar and amphibole may be present.

The distribution of intrusions is not well correlated with measured temperatures, suggesting that intrusive activity has occurred in the area over the past several million years. A NW-trending band of high temperatures parallel to the axis of arc volcanism and the general trend of the Philippine Fault appears to mark the area of the youngest intrusions. Young silicic volcanism (<22,000 years old) and high temperatures (up to 350°C) at 2.5 to 3.5 km depth suggest that the most recent subvolcanic intrusions are providing the heat sustaining hydrothermal circulation.

cap and first appearance of epidote (Figs. 3A and 4), which marks the approximate top of the reservoir, generally followed the present-day isotherms. Smectite occurs in the upper part of the cap; at greater depths interlayered illite-smectite and chlorite-smectite are present. Blocky, equant calcite is mainly found at shallow levels within the clay cap, but it is also abundant on the E (e.g., Bul-34) and S margins of the commercial reservoir, and along the margins of the production zone (Figure 3B). For example, it is very abundant in Bul-19 from about -1200 to -2300 m asl, where it fills voids and veins, and partially replaces feldspar.

The SE sector of Bulalo is a distinctive zone of fluid chemistry and rock alteration (Clemente, 1987). It is characterized by abundant calcite compared to the remainder of the production area, similar in some regards to outfield areas of

Table 1. Distribution of intrusive rocks and associated hydrothermal alteration.

Well	Area	Depth (m)	Intrusion Type	Associated alteration
			OUTFIELD	
19	SE	182 to 244	Fn gr basaltic dike/sill	Argillic
		1158 to 1219	Diabase and other fn gr dike/sill	Weak Propylitic
		2622 to 2743	Diabase and other dike/sill	Propylitic
25		975	Pyx microdiorite	Propylitic
		1220 to 1646	Pyx microdiorite	Propylitic
31A	NE	2110 to 2115	Fn gr gabbro	Propylitic
77		2362 to 2365	Med gr diorite	Propylitic
94		2845 to 2847	Pyx-hb diorite	Potassic
82		2873 to 2876	Microdiorite	Propylitic
69	SW	1645 to TD	Fn gr dike/sill	Phyllic/Propylitic/local AA
68		2470	Fn gr dike/sill	Propylitic
		3475 to 3624	Pyx-bt granodiorite	Potassic/Phyllic
85	Far SW	2560, 2804	Fn gr to cr gr hb-diorite	Propylitic
		3006 to 3009	Fn gr diorite	Propylitic
87		2165, 2315-2345	Fn gr intrusion	Phyllic/Propylitic
45	W	2134 to 2317	Microdiorite	Propylitic/Phyllic
58		1280, 1435	Granodiorite	Phyllic
75		2560	Fn gr dike/sill	Phyllic
		2621 to 2682	Pyx microdiorite	Phyllic
81	Far NW	2469 to 2682	Fn gr dike/sill	Phyllic/Propylitic
		2804 to 3048	Microdiorite	Propylitic/Phyllic
			INFIELD	
17	S AND SE	2164, 2256	Qtz dacite dike, microdiorite	
22		1035 to 1160	Fn gr pyx microdiorite dike/sill	Potassic hornfels
46		1830 to 2135	Microdiorite dike/sill	Potassic hornfels
53		2487, 2792	Microdiorite dike/sill	Propylitic
55		2743 to 2848	Med gr bt granodiorite	Propylitic
83		2195, 2260	Qtz dacite, microdiorite dike/sill	Propylitic
92		2113 to 2116	Microgabbro	Propylitic
65	W	2745	Pyx monzonite	Weak Propylitic
108	NW	2887 to 2918	Fn gr to med gr pyx diorite	Propylitic
34	NE	305, 335, 488	Dacite dike/sill	Weak argillic
		2317	Pyx diorite	Phyllic/Propylitic

Abbreviations: AA = advanced argillic; bt = biotite; cr gr = coarse grained; fn gr = fine grained; hb = hornblende; med gr = medium grained; pyx = pyroxene; qtz = quartz.

Vein Paragenesis and Fluid Inclusions

The vein assemblages can be broadly grouped into two distinct parageneses that formed at different times in the evolution of the hydrothermal system (Figure 5). The earliest hydrothermal vein assemblages are characterized by calcite, chalcedony and quartz (Figure 5A) or the propylitic assemblage epidote, chlorite, pyrite, chalcedony and quartz (Figure 5B). Prehnite, actinolite, garnet, albitic plagioclase and potassium feldspar may also be locally present but are relatively uncommon despite fluid inclusion evidence that temperatures had exceeded 300°C during formation of the propylitic assemblages.

Silica deposited as chalcedony can be recognized by the presence of botryoidal or colloform textures (Figure 5). In places, botryoidal textures outlined by small fluid inclusions are preserved within the cores of euhedral quartz crystals indicating that silica deposition was initiated with the precipitation of chalcedony.

The formation of paragenesis 1 was followed by the deposition of calcite, anhydrite (Figure 5) and wairakite, which was locally accompanied by quartz and chlorite. Anhydrite and calcite deposited during paragenesis 2 typically form monomineralic veins and vug fillings.

Homogenization temperatures and salinities were determined on more than 800 fluid inclusions trapped in epidote, quartz, anhydrite and calcite (J. Reynolds, unpub. data and this study). The inclusions were classified as primary or secondary based on petrographic criteria. Only two phase liquid- and vapor-rich inclusions were observed with liquid-rich inclusions dominating the fluid inclusion population. Heating and freezing measurements were only made on the liquid-rich inclusions. Homogenization temperatures and salinities (wt% NaCl equivalent) of inclusions trapped in epidote ranged from 265-350° (avg. 316°C) and 0-3.5 wt% (avg. 1.6 wt%), in quartz from 240-345° (avg. 295°C) and 0-0.2 wt% (avg. 0.5 wt%), in calcite from 182-345° (avg. 266°C) and 0-4.2 wt% (avg. 0.7 wt %) and in anhydrite from 251-318°C (avg. 278°C) and 0.5-1.9 wt% (avg. 1.2 wt%). Figure 4 compares the fluid inclusion and measured temperatures in the northern part of the field.

Discussion and Conclusions

Detailed investigations of the mineral parageneses and the fluid inclusions trapped in hydrothermal minerals record a complex thermal history. The early history of the Bulalo geothermal system is represented by vein assemblages dominated by either calcite or epidote. Fluid inclusions trapped in epidote typically record temperatures exceeding 300°C. These temperatures follow a boiling point to depth curve that intersects the present surface. Fluids trapped in later quartz were less saline and generally slightly lower in temperature,
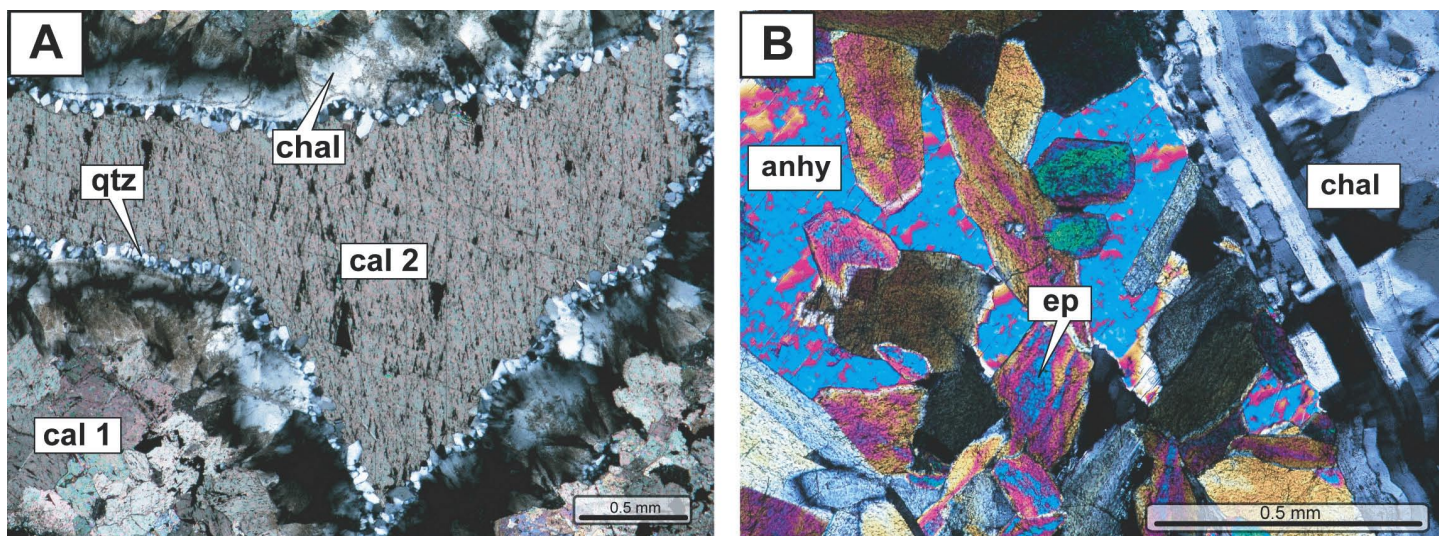
Figure 5. Photomicrographs showing Bulalo vein parageneses. The images were taken under crossed nicols. (A) Sequential deposition of calcite (cal 1), chalcedony (chal) and quartz (qtz) representative of paragenesis 1, with later deposition of calcite (cal 2) representative of paragenesis 2. Homogenization temperatures of quartz-hosted fluid inclusions ranged from 340-345°C; those in calcite 2 averaged 329°C and had an average salinity of 0.8 wt% NaCl equivalent. Sample from Bul-19 at -2097 m asl. (B) Photomicrograph of epidote (ep) and later anhydrite (anhy) filling a vug in a chalcedony vein. Homogenization temperatures and salinities of fluid inclusions in anhydrite average 310°C and 1.6 wt% NaCl equivalent respectively. Epidote and chalcedony were deposited during paragenesis 1; anhydrite during paragenesis 2. Sample from Bul-92 at -1835 m asl.

suggesting increased mixing with more dilute and slightly cooler waters.

The field wide deposition of chalcedony during paragenesis 1 provides evidence of a significant pressure change during the evolution of the system. Although chalcedony is typically not a stable phase at temperatures exceeding ~180°C (Fournier, 1985), its occurrence with epidote and the homogenization temperatures of fluid inclusions trapped in associated calcite and anhydrite (refer to Figure 5) indicate that deposition of chalcedony occurred at temperatures exceeding 300°C. At temperatures >235°C, extreme oversaturation of silica with respect to quartz is required before chalcedony will precipitate (Fournier, 1985). The most likely cause of oversaturation is decompression and boiling. Moore et al. (2004a) demonstrated that the formation of chalcedony at similar temperatures at Karaha-Telaga Bodas, Indonesia resulted from catastrophic decompression and boiling during flank collapse of Galung-gung Volcano. No extraordinary volcanic eruptions are known to have occurred in the recent past at Bulalo. Thus, decompression was most likely associated with the emplacement of the dacite domes, the youngest recognized volcanic event within the last 22,000 years. Although decompression at Karaha-Telaga Bodas triggered formation of the modern-vapor-dominated regime, no evidence for extensive boiling off of the fluids is found at Bulalo. Higher marginal permeabilities at Bulalo may have allowed rapid recharge of the system that limited progressive boiling to vapor-dominated conditions.

As the peak temperatures and fluid outflow waned, sulfate- and carbonate-rich fluids descended or moved laterally into the hotter rocks, depositing anhydrite or calcite because of their retrograde solubilities (paragenesis 2). The clay cap expanded downward, overprinting the early deposited epidote in the distal parts of the system. Wairakite, which is frequently associated with anhydrite or calcite, formed at depth where these slightly acidic waters mixed with the in-situ reservoir fluids (e.g. Moore et al., 2004b). In general, the temperatures recorded by fluid inclusions trapped in calcite and anhydrite are consistent with the measured temperatures, suggesting the present thermal regime developed in the recent past.

Acknowledgements

References

Abrigo, F.V., Molling, P.A., and J.A. Acuña, 2004. "Determination of recharge and cooling rates using geochemical constraints at the Mak-Ban (Bulalo) geothermal reservoir, Philippines." Geothermics, v. 33, p. 11-36.

Clemente, W.C., 1987. "Petrographic Study of Mak-Ban Geothermal Field." Unpublished Philippine Geothermal, Inc. Report.

Clemente, W.C., and F.L. Villadolid-Abrigo, 1993. "The Bulalo geothermal field, Philippines: reservoir characteristics and response to production." Geothermics v. 22, p. 381-394.

Dimabuyu, A.C., Stimac, J.A., Aquino, D., and J. Lowenstern, 2005. "A time-calibrated volcanic facies model for the Bulalo geothermal field, Philippines." Proceedings AGU Chapman Conference on Volcano-Tectonic Interactions, Tagaytay, Philippines.

Förster, H., Oles, D, Knittel, U., Defant, M.J., and R.C. Torres, 1990. "The Macolod Corridor: A rift crossing the Philippine island arc." Tectonophysics, v. 183, p. 265-271.

Fournier, R.O., 1985. "The behavior of silica in hydrothermal solutions." In Geology and Geochemistry of Epithermal Systems: Reviews in Economic Geology (B.R. Berger & P.M. Bethke, eds.). Reviews in Economic Geology, v. 2, p. 45-62.

Golla, G.U., Abrigo, F., Alarcon, B.O., Molling, P.A., and J. and Stimac, 2001. "The Bulalo geothermal field, Philippines: Conceptual model of a prolific geothermal system." Proceedings 22nd PNOC-EDC Conference on Geothermal Energy, p. 123-132.

Hedenquist, J.W., Arribas, A. Jr., and T.J. Reynolds, 1998. "Evolution of an intrusion-centered hydrothermal system: Far Southeast-Lepanto porphyry and epithermal Cu-Au deposits, Philippines." Economic Geology, v. 93, p. 373-404.

Hilton, D.R., Fischer, T.P., Stimac, J.A., and D.D. Leeuw, 2004. "The importance of source composition on the carbon output of the Luzon and Bicol arcs, the Philippines." Proceedings, IAVCEI General Assembly, Pucon, Chile.

Hochstein, M., and P.R.L. Browne, 2000 "Encyclopedia of Volcanoes." Sigurdsson (ed.), Academic Press, 1417p.

Moore, J. N., Christenson, B., Browne, P. R. L. and S. Lutz, 2004a. "The mineralogic consequences and behavior of descending acid-sulfate waters: an example from the Karaha-Telaga Bodas geothermal system, Indonesia." Canadian Mineralogist, v. 42, p. 1483-1499.

Moore, J., Bruton, C. and T. Powell, 2004b. "Wairakite: A potential indicator of fluid mixing." Geothermal Resources Council Transactions, v. 28, p. 495-498.

Reyes, A.G., 1990 "Petrology of Philippine geothermal systems and the application of alteration mineralogy to their assessment." Journal of Volcanology and Geothermal Research, v. 43, p. 279-309.

Vogel, T.A., Flood, T.P., Patino, L.C., Wilmot, M.S., Maximo, R.P.R., Arpa, C.B., Arcilla, C.A., and J.A. Stimac, 2006. "Geochemistry of silicic magmas in the Macolod Corridor, SW Luzon, Philippines: evidence of distinct, mantle derived, crustal sources for silicic magmas." Contributions to Mineralogy and Petrology. v. 151, p. 267-281.